

Audio Spectral Enhancement: Leveraging Autoencoders for Low Latency Reconstruction of Long, Lossy Audio Sequences

Darshan Deshpande

DARSHAN.DESHPANDE_STUDENT@THADOMAL.ORG

*Department of Computer Engineering
Thadomal Shahani Engineering College
Mumbai University
Mumbai, India.*

Harshavardhan Abichandani

HARSHAVARDHAN.ABICHANDANI_STUDENT@THADOMAL.ORG

*Department of Computer Engineering
Thadomal Shahani Engineering College
Mumbai University
Mumbai, India.*

Editor:

Abstract

With active research in audio compression techniques yielding substantial breakthroughs, spectral reconstruction of low-quality audio waves remains a less indulged topic. In this paper, we propose a novel approach for reconstructing higher frequencies from considerably longer sequences of low-quality MP3 audio waves. Our technique involves inpainting audio spectrograms with residually stacked autoencoder blocks by manipulating individual amplitude and phase values in relation to perceptual differences. Our architecture presents several bottlenecks while preserving the spectral structure of the audio wave via skip-connections. We also compare several task metrics and demonstrate our visual guide to loss selection. Moreover, we show how to leverage differential quantization techniques to reduce the initial model size by more than half while simultaneously reducing inference time, which is crucial in real-world applications.

Keywords: Audio Reconstruction, Audio Enhancement, Autoencoders, Quantization, Short-Time Fourier Transform

1. Introduction

Data compression is utilised in a variety of ways, from streaming music to transferring text files, but it has had the greatest impact on the audio and image domains. Among all audio compression algorithms, MP3 is a well-known codec, primarily because it drastically decreases the file size while having little effect on audio quality. It uses a perceptual model which removes frequencies that are imperceptible to humans, usually involving the high frequencies. The way it does this is by changing the input from the time domain to the frequency domain by using FFT and subsequently determining the threshold values of these frequencies. After this, Huffman encoding is applied to further compress the file by assigning lower number of bits to the frequently occurring frequencies. MP3 is a lossy compression format since it removes information from the audio that is difficult to recover. The loss

of information is not perceptible by humans at high enough bitrates, but at low bitrates artifacts like pre-echo are noticeable.

Some techniques have been established previously, in which the algorithm would iteratively estimate the phase source and reconstruct the audio (Gunawan and Sen, 2010; Mowlae et al., 2012; Krawczyk and Gerkmann, 2014). These techniques of estimating the phase show considerable improvement in the SSNR and PESQ score, but all of them ignore other characteristics of the audio like the magnitude and power spectrum (Tan and Wang, 2019). In recent times machine learning methods have been used to outperform these algorithmic techniques. CNN models were utilised, with the real and imaginary spectrograms of the audio serving as separate input channels for the model (Fu et al., 2017). The resultant spectrograms were then used for the reconstruction of the signal, this type of reconstruction outperformed the algorithmic approaches.

Convolutional Recurrent Neural Network (CRN) model proposed by (Tan and Wang, 2019) had a substantially higher STOI and PESQ value compared to the CNN based approach mentioned above (Fu et al., 2017). Later, (Kuleshov et al., 2017) proposed a technique in which time-series data is fed into an autoencoder with residual connections, which reconstructs the high resolution audio with a sampling rate higher than the low resolution audio. This model was inspired by the image super resolution paper (Dong et al., 2016) and demonstrates an improvement of about 5dB in some circumstances (Kuleshov et al., 2017). Resnet and Unets (Sulun and Davies, 2021) have also been tested for the task of bandwidth extension. Multiple low pass filters were utilised to enhance the data, allowing these models to generalize effectively on new unseen filters (Sulun and Davies, 2021). The code for the sections that follow can be found at: <https://github.com/DarshanDeshpande/audio-spectral-enhancement>.

2. Processing the Data

The usage of extended temporal sequences is the fundamental focus of our research (above 100,000 data points per training sample). Because of the limited input size and repeated sweeps of segments through the decoder network that are necessary to rebuild lengthier audio sequences, upscaling with some previous reconstruction algorithms like (Pascual et al., 2017) is significantly slower. Although parallelism helps speed up the process, larger audio files still take a long time to process. To help mitigate this major constraint, one of the most practical solutions is to analyse and reconstruct larger audio sequences in a single inference which is what we use for our proposed model. This section provides details about the creation of training data and the structuring of the pipeline.

2.1 Dataset

We use the GTZAN (Tzanetakis and Cook, 2002) dataset as a base for our experiments. It includes 1,000 WAV tracks, each of which lasts 30 seconds and are sampled at 22050 Hz. Each of these songs was divided into three parts, augmenting the total number of songs in the dataset to 3,000. Using the LAME encoder (Cheng, 1998) and the FFmpeg library (Tomar, 2006), all 3,000 mono 16bit WAV files were first converted to MP3 files at a constant bitrate of 128kbps. We then downsampled the 128kbps audio files to 32kbps audio

files using the same LAME encoder and the FFmpeg library (Tomar, 2006). We have used 85% of the data for training, 8% data for validation and 7% data for testing.

2.2 Loading the Data

To accurately capture the differences between high and low bitrate audio, the data was preprocessed using the Short Time Fourier Transform (STFT). The STFT function returns a tensor of complex STFT values containing information about the signal’s phase and amplitude, which was then separated into real and imaginary parts and stacked on top of each other. Stacking was done because the real and imaginary values are directly mappable to the new real and imaginary values, respectively.

We experimented with various frame length and hop size configurations to retrieve the most data while minimizing processing time. We found that a Hanning window length of 1023, hop size of 248, a frame length of 1024 without padding or centering provided the best results. This configuration gives us 400 frames and 512 frequency bins for every sample of 100,000 data points. The hop size should be small and the frame length should be large to achieve accurate inversion. Lowering the hop size to a very small value increases the time resolution but it is very computationally heavy. This leads to increased inference time and as a result, our setup finds a good compromise between the two.

3. Model Creation

Popular purely convolutional networks such as ResNets (He et al., 2016) and UNets (Ronneberger et al., 2015), rely heavily on residual connections and lower dimensional projections. When training data is scarce and fast inference is of high priority, our experiments revealed that these large models are significantly less efficient. In our study, we found that 2-D Convolutional UNets (Ronneberger et al., 2015) consistently produced poor latent representations, drawing more attention to the background noise instead of the missing frequencies. Furthermore, 1-D UNet based models like Wave-U-Net (Stoller et al., 2018), Temporal FiLM (Birnbaum et al., 2019) and Audio-SR-Net (Sulun and Davies, 2021) have only been tested for sequences with 10,000 or fewer data points per sample. We discovered that 1-D convolutions applied to training samples temporally ten times that size are extremely inefficient and computationally costly to train. The subsections that follow detail the experiments and model designs that were employed.

3.1 Model Architecture

Since one-dimensional models are unusable as discussed above, it is more cost and time effective to directly convolve on the stacked STFT output. Previously mentioned 2-D UNet architecture (Ronneberger et al., 2015) was designed with a fixed positive range of 0 to 1 for images in mind. Since we had to scale our data in order to feed it to the 2-D UNet model (Ronneberger et al., 2015), we had two options for dealing with the issue of negative values in the scaled data: the first was to change the range of our data to 0 to 1, and the second was to use activation functions like *tanh*, which support negative values. In comparison to the first method, which resulted in insufficient weighting of negative values, our comparative trials demonstrated that the second strategy resulted in significantly improved spectral

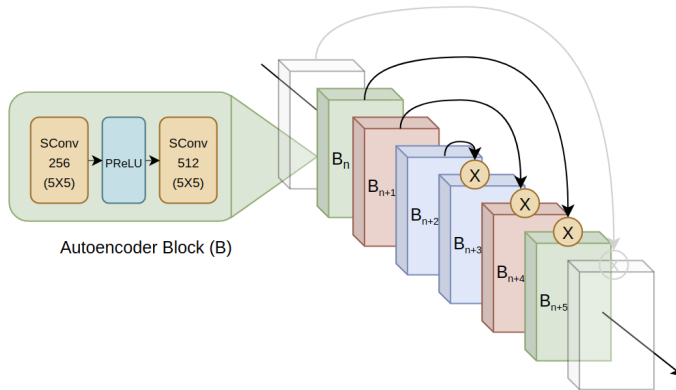


Figure 1: A single Depthwise Separable Convolution Block(B) and it’s arrangement as a residually connected autoencoder network

structure retention. Both the PReLU (He et al., 2015) and \tanh functions work well with the 2-D U-Net (Ronneberger et al., 2015), but they quickly overfit due to the large number of trainable parameters and small dataset size, resulting in an extremely saturated spectral plot and poor audio output.

Our proposed model consists of a two-layer 2-D depthwise separable convolutional (Sifre and Mallat, 2014) block, as seen in figure 1. This architecture functions as a tiny autoencoder unit with a 256-dimensional latent space. Each block uses a PReLU (He et al., 2015) activation which prevents the gradients from exploding while performing significantly better than \tanh function in our experiments. With PReLU (He et al., 2015) and α parameter initialization of zero, the model attains more freedom to explore negative values which is not possible with the standard ReLU or sigmoid activation functions. This activation function is sandwiched between separable convolutional layers (Sifre and Mallat, 2014), each with a filter size of 5×5 and step size of 1. Our model uses constant padding which persists the input rows in the output, along with a randomly uniform initialization in accordance with the initialization proposed by (He et al., 2015). The use of separable convolutions (Sifre and Mallat, 2014) rather than general spatial convolutions stems from their low likelihood of overfitting (Sifre and Mallat, 2014), as demonstrated by our experiments with considerably higher trainable parameters and various custom experiments that are shown in table 1. Each block can be stacked N times with skip connections as shown in figure 1 to provide effective protection against the vanishing gradient problem (He et al., 2016). A significant observation is that with the increase of N , the coherence of the output audio decreases despite the phase and power spectra remaining consistent. Through our experiments, we could also conclude that a model consisting upto seven autoencoder blocks does not lead to overfitting on our experiments with our augmented GTZAN dataset (Tzanetakis and Cook, 2002). This explains the robust architectural design of the configuration primarily due to the use of separable convolutions (Sifre and Mallat, 2014).

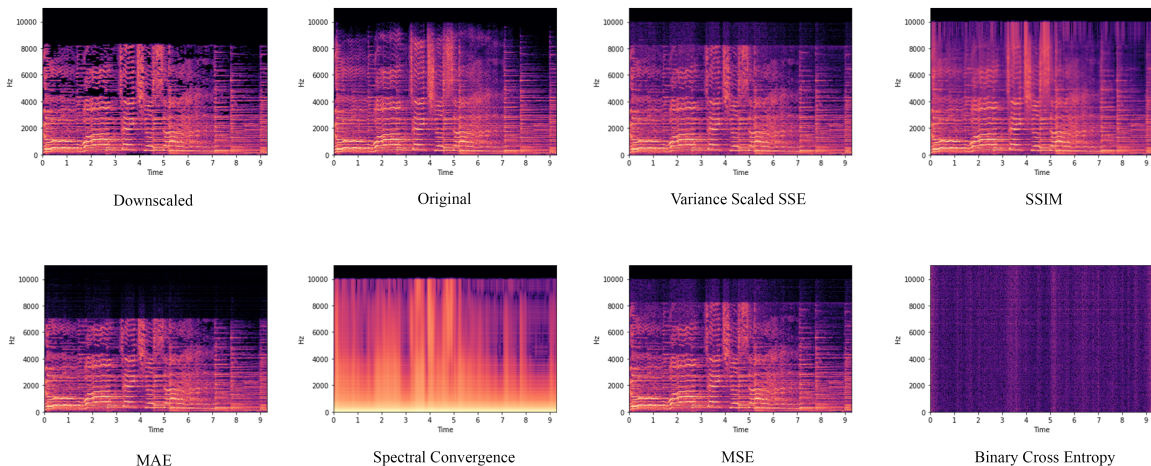


Figure 2: Outputs of different loss functions

3.2 Training Losses

Our experimentation with loss functions involved permuting between six losses and testing their combinations. The figure 2 provides a summary of the individual metric tests. Considering these effects, we propose a weighted combination of two losses for our training process. First is a modified version of the sum of squared residuals (SSE) which is scaled by the variance of the ground truth label.

$$\text{Pixel Loss}(y_i, \hat{y}_i) = \frac{\sum_{i=1}^n (y_i - \hat{y}_i)^2}{\sum_{i=1}^n (y_i - \bar{y})^2} \quad (1)$$

This loss function provides a much better spectral structure as compared to the standard Mean Squared Error (MSE) for unscaled data or Kullback-Leibler Divergence (KDL) for scaled data which produced faded textures. Similarly, Mean Absolute Error (MAE) produced results that neglected the higher frequencies altogether because of its inherent nature of ignoring outliers. Some commonly employed spectral reconstruction losses, such as Log Spectral Loss (Hu and Loizou, 2008), resulted in oversaturated low-frequency regions that were not affected by compression, to begin with, as seen in figure 2.

The second loss that we use is the Structural Similarity Index (SSIM) (Wang et al., 2004). The idea for this function is derived from its large applicability in domains such as image reconstruction and image super-resolution. SSIM highly influences the spectral luminosity and contrast of the output spectrogram and ensures that the higher frequency intensity ranges are equally stressed on unlike the Log Spectral Loss (Hu and Loizou, 2008)

$$\text{SSIM}(y_i, \hat{y}_i) = \frac{(2\mu_{y_i}\mu_{\hat{y}_i} + C_1)(2\sigma_{y_i\hat{y}_i} + C_2)}{(\mu_{y_i}^2 + \mu_{\hat{y}_i}^2 + C_1)(\sigma_{y_i}^2 + \sigma_{\hat{y}_i}^2 + C_2)} \quad (2)$$

Here, the SSIM loss is calculated on the magnitude of the output. $C_1 = (k_1L)^2$ and $C_2 = (k_2L)^2$ are constants for stabilization determined by the dynamic pixel value ranges, L , and pre-determined constants k_1, k_2 . Changing the value of k_1 even slightly, changes the luminosity by a large factor and hence this value is most optimal if set between 0.01 and

0.005. Additionally, altering the value of k_2 gives a better definition to the output spectral plot at the cost of low intensity of higher frequencies. Thus, the appropriate value of k_2 can range from 0.01 to 0.03. The value of L should be set to less than $1/2$ of the actual pixel range to allow for better luminosity. (Wang et al., 2004) recommend that the technique should be applied locally for better results. Our exhaustive experiments conclude that applying the loss using a smaller convolutional window size of 3×3 improves the structural detail of the output and prevents checkerboard patterns.

3.3 Training

The training process involves using the Adam (Kingma and Ba, 2014) optimizer and takes approximately 200 epochs to converge with a learning rate of 1×10^3 and a mini batch size of 32. Other popular optimizers, such as mini-batch SGD and RMSProp, are prone to get trapped in local minima, resulting in insufficient loss landscape mapping. The training time heavily depends on the model configuration, number of parameters and the value of N mentioned in subsection 3.1. Additionally, a cyclical learning rate with a decay factor of 5×10^{-4} can assist in providing a smoother descent.

At every step, the losses are weighted as follows:

$$\text{Total Loss} = \text{Pixel Loss} + 0.5 \times \text{SSIM} \quad (3)$$

This weighting is used to counteract SSIM’s tendency to dominate the spectrogram by filling it with unnecessary high-intensity pixels. This prevents the spectrogram from being overly saturated and producing a noisy audio output.

3.4 Model Quantization

Since the primary goal of this research is to provide a low latency solution for spectral mapping, we adopt quantization techniques (Jacob et al., 2018) to shrink the model size as well as decrease inference times. We used a dynamic 8-bit precision quantization to achieve a compression of up to 52.15%, resulting in a compressed size of 956KB per block. In this quantization technique, the activations are dynamically quantized and un-quantized between 8-bit and float precisions during and after training respectively, while the weights are stored with 8-bit precision. The differences in spectrograms after compression is minuscule, with 16-bit float quantization techniques retaining the complete spectral structure and the 8-bit integer quantization techniques altering the intensity of the higher frequencies just slightly, while ensuring the persistence of the quality of the audio output.

4. Evaluation

The evaluation section is divided into two parts. First, the spectrograms of high, low and approximated audio signals are compared and finally, some of the most common objective and perceptual based metrics are used to evaluate the audio signals.

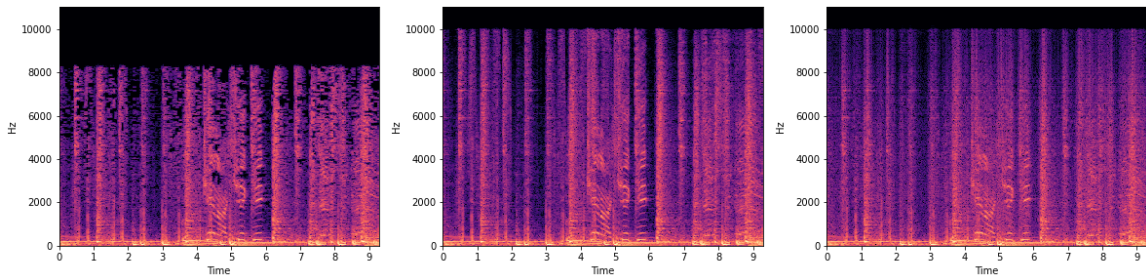


Figure 3: From left to right: low bitrate audio spectrogram, high bitrate audio spectrogram and reconstructed audio spectrogram

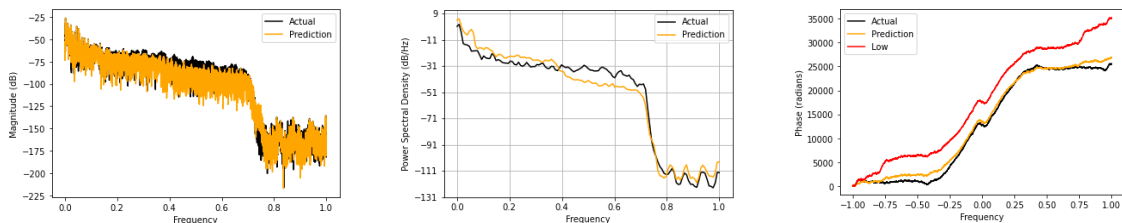


Figure 4: From left to right: magnitude spectrogram, power spectrogram and two-sided phase spectrogram

4.1 Spectrograms

Inverse STFT of the approximated signal was taken and then its frequency, phase, magnitude and power spectrograms were plotted against the high bitrate audio signal as shown in figure 4. Figure 3 shows that the reconstructed spectrogram has kept the structure of higher frequencies. Figure 4 shows a two-sided phase spectrogram that displays how the reconstructed phase differs just slightly from the high bitrate audio.

4.2 Metrics

The performance of the reconstructed audio signal \hat{y} in comparison to the high bitrate audio signal y was evaluated using the following metrics.

1. Signal to Noise Ratio (SNR)

$$\text{SNR}(y, \hat{y}) = 10 \cdot \log_{10} \frac{\|y\|_2^2}{\|y - \hat{y}\|_2^2} \quad (4)$$

Signal to Noise ratio is the most widely used metric for analyzing the clarity of the audio signals. The higher the value of the ratio, the better is the audio quality.

2. Perceptual Evaluation of Speech Quality (PESQ)

It is calculated by taking the linear combination of the average disturbance values D_{ind} and the average asymmetrical disturbance values A_{ind} (Hu and Loizou, 2008;

Rix et al., 2001).

$$\text{PESQ}(y, \hat{y}) = a_0 + a_1 D_{ind} + a_2 A_{ind} \quad (5)$$

We have taken all the default values of a_0 , a_1 , and a_2 and used a wideband configuration with the sampling frequency of 16000Hz as mentioned in (Wang, 2021).

3. Log-Spectral Distance (LSD)

$$\text{LSD}(y, \hat{y}) = \frac{1}{L} \sum_{l=1}^L \sqrt{\frac{1}{K} \sum_{k=1}^K (S(k) - \hat{S}(k))^2} \quad (6)$$

here S and \hat{S} are calculated by first taking the STFT of y and \hat{y} respectively (Gray and Markel, 1976). For the STFT, a window length of 2048 was chosen, followed by the log of the square of absolute values of the STFT. Here K and L represents the frequencies and the total number of frames respectively.

4. Short-Time Objective Intelligibility (STOI)

STOI was calculated based on the parameters mentioned in (Taal et al., 2010, 2011) with the high bitrate audio, the reconstructed audio and the sampling rate equal to 44100Hz as the inputs to the function.

Table 1: Inference time in milliseconds and metric comparison of different models.

	Audio-SR-Net (27.7ms)	FFmpeg	TFiLM (75.9ms)	WaveNet (86.9ms)	N = 1 (7.74ms)	N = 5 (20.8ms)
SNR	16.7353	18.0077	9.9723	13.6910	21.2532	20.8868
PESQ	2.6296	4.3039	3.6352	4.1743	4.3599	4.1197
LSD	2.3340	2.6845	2.6497	3.1490	1.5909	1.8152
STOI	0.9996	0.9913	0.9635	0.9881	0.9910	0.9894

In table 1, a single autoencoder block ($N = 1$) outperforms the majority of the models compared. Even though it contains six times the number of trainable parameters as a single block, the five block autoencoder ($N = 5$) shows a slight variation in metric values and does not overfit. This demonstrates that a small sized model is adequate to generalize and is sufficiently robust that, when the size is increased, it shows no major evidence of overfitting when compared to the other techniques.

5. Conclusion and Improvements

In this paper, we propose a novel architecture involving nested, residually connected autoencoder blocks for the spectral reconstruction of monaural audio samples. The preprocessing pipeline involves the conversion of a higher, 128Kbps audio wave to a lower, 32Kbps audio using FFmpeg (Tomar, 2006) whose reconstruction was then attempted using the residual network. We compare our method against FFmpeg (Tomar, 2006) based reconstruction

and a variety of preexisting and new machine learning methods using popular perceptual metrics such as PESQ (Rix et al., 2001) and LSD (Gray and Markel, 1976). Furthermore, we discuss how the proposed model can be pruned to a minimum size of 956KB (52.15%) per autoencoder block, resulting in perceptually comparable inferences.

Despite the benefits of the architecture and techniques used, the output wave sometimes tends to be slightly incoherent with the source. Furthermore, due to a lack of open sourced trainable data, the model could only be trained on 3,000 samples, resulting in poor generalisation of the silent regions in the audio spectra. Additionally, Generative Adversarial Networks (GANs) (Goodfellow et al., 2014) and Audio Transformers (Gong et al., 2021), and the use of coherence-based comparative metrics are two noteworthy approaches to consider for future trials.

References

- Sawyer Birnbaum, Volodymyr Kuleshov, S. Enam, Pang Wei Koh, and S. Ermon. Temporal film: Capturing long-range sequence dependencies with feature-wise modulations. In *NeurIPS*, 2019.
- Mike Cheng. LAME MP3 Encoder, 1998. URL <https://lame.sourceforge.io/>.
- Chao Dong, Chen Change Loy, Kaiming He, and Xiaoou Tang. Image super-resolution using deep convolutional networks. *IEEE Transactions on Pattern Analysis and Machine Intelligence*, 38(2):295–307, 2016. doi: 10.1109/TPAMI.2015.2439281.
- Szu-Wei Fu, Ting-yao Hu, Yu Tsao, and Xugang Lu. Complex spectrogram enhancement by convolutional neural network with multi-metrics learning. In *2017 IEEE 27th International Workshop on Machine Learning for Signal Processing (MLSP)*, pages 1–6, 2017. doi: 10.1109/MLSP.2017.8168119.
- Yuan Gong, Yu-An Chung, and James R. Glass. AST: audio spectrogram transformer. *CoRR*, abs/2104.01778, 2021. URL <https://arxiv.org/abs/2104.01778>.
- Ian Goodfellow, Jean Pouget-Abadie, Mehdi Mirza, Bing Xu, David Warde-Farley, Sherjil Ozair, Aaron Courville, and Yoshua Bengio. Generative adversarial nets. *Advances in neural information processing systems*, 27, 2014.
- A. Gray and J. Markel. Distance measures for speech processing. *IEEE Transactions on Acoustics, Speech, and Signal Processing*, 24(5):380–391, 1976. doi: 10.1109/TASSP.1976.1162849.
- David Gunawan and D. Sen. Iterative phase estimation for the synthesis of separated sources from single-channel mixtures. *IEEE Signal Processing Letters*, 17(5):421–424, 2010. doi: 10.1109/LSP.2010.2042530.
- Kaiming He, Xiangyu Zhang, Shaoqing Ren, and Jian Sun. Delving deep into rectifiers: Surpassing human-level performance on imagenet classification. In *Proceedings of the IEEE international conference on computer vision*, pages 1026–1034, 2015.

- Kaiming He, Xiangyu Zhang, Shaoqing Ren, and Jian Sun. Deep residual learning for image recognition. In *Proceedings of the IEEE conference on computer vision and pattern recognition*, pages 770–778, 2016.
- Yi Hu and Philippos C. Loizou. Evaluation of objective quality measures for speech enhancement. *IEEE Transactions on Audio, Speech, and Language Processing*, 16(1):229–238, 2008. doi: 10.1109/TASL.2007.911054.
- Benoit Jacob, Skirmantas Kligys, Bo Chen, Menglong Zhu, Matthew Tang, Andrew Howard, Hartwig Adam, and Dmitry Kalenichenko. Quantization and training of neural networks for efficient integer-arithmetic-only inference. In *Proceedings of the IEEE conference on computer vision and pattern recognition*, pages 2704–2713, 2018.
- Diederik P Kingma and Jimmy Ba. Adam: A method for stochastic optimization. *arXiv preprint arXiv:1412.6980*, 2014.
- Martin Krawczyk and Timo Gerkmann. Stft phase reconstruction in voiced speech for an improved single-channel speech enhancement. *IEEE/ACM Transactions on Audio, Speech, and Language Processing*, 22(12):1931–1940, 2014. doi: 10.1109/TASLP.2014.2354236.
- Volodymyr Kuleshov, S. Zayd Enam, and Stefano Ermon. Audio super resolution using neural networks, 2017.
- Pejman Mowlae, Rahim Saeidi, and Rainer Martin. Phase estimation for signal reconstruction in single-channel source separation. In *Thirteenth Annual Conference of the International Speech Communication Association*, 2012.
- Santiago Pascual, Antonio Bonafonte, and Joan Serra. Segan: Speech enhancement generative adversarial network. In *Proc. Interspeech 2017*, pages 3642–3646, 2017. doi: 10.21437/Interspeech.2017-1428. URL <http://dx.doi.org/10.21437/Interspeech.2017-1428>.
- A.W. Rix, J.G. Beerends, M.P. Hollier, and A.P. Hekstra. Perceptual evaluation of speech quality (pesq)-a new method for speech quality assessment of telephone networks and codecs. In *2001 IEEE International Conference on Acoustics, Speech, and Signal Processing. Proceedings (Cat. No.01CH37221)*, volume 2, pages 749–752 vol.2, 2001. doi: 10.1109/ICASSP.2001.941023.
- Olaf Ronneberger, Philipp Fischer, and Thomas Brox. U-net: Convolutional networks for biomedical image segmentation. In Nassir Navab, Joachim Hornegger, William M. Wells, and Alejandro F. Frangi, editors, *Medical Image Computing and Computer-Assisted Intervention – MICCAI 2015*, pages 234–241, Cham, 2015. Springer International Publishing. ISBN 978-3-319-24574-4.
- Laurent Sifre and Stéphane Mallat. Rigid-motion scattering for texture classification, 2014.
- D. Stoller, S. Ewert, and S. Dixon. Wave-u-net: A multi-scale neural network for end-to-end audio source separation. *ArXiv*, abs/1806.03185, 2018.

- Serkan Sulun and Matthew E. P. Davies. On filter generalization for music bandwidth extension using deep neural networks. *IEEE Journal of Selected Topics in Signal Processing*, 15(1):132–142, 2021. doi: 10.1109/JSTSP.2020.3037485.
- Cees H. Taal, Richard C. Hendriks, Richard Heusdens, and Jesper Jensen. A short-time objective intelligibility measure for time-frequency weighted noisy speech. In *2010 IEEE International Conference on Acoustics, Speech and Signal Processing*, pages 4214–4217, 2010. doi: 10.1109/ICASSP.2010.5495701.
- Cees H. Taal, Richard C. Hendriks, Richard Heusdens, and Jesper Jensen. An algorithm for intelligibility prediction of time–frequency weighted noisy speech. *IEEE Transactions on Audio, Speech, and Language Processing*, 19(7):2125–2136, 2011. doi: 10.1109/TASL.2011.2114881.
- Ke Tan and DeLiang Wang. Complex spectral mapping with a convolutional recurrent network for monaural speech enhancement. In *ICASSP 2019 - 2019 IEEE International Conference on Acoustics, Speech and Signal Processing (ICASSP)*, pages 6865–6869, 2019. doi: 10.1109/ICASSP.2019.8682834.
- Suramya Tomar. Converting video formats with ffmpeg. *Linux Journal*, 2006, 06 2006.
- G. Tzanetakis and P. Cook. Musical genre classification of audio signals. *IEEE Transactions on Speech and Audio Processing*, 10(5):293–302, 2002. doi: 10.1109/TSA.2002.800560.
- Wang. GitHub - ludlows/python-pesq: PESQ (Perceptual Evaluation of Speech Quality) Wrapper for Python Users (narrow band and wide band), 2021. URL <https://github.com/ludlows/python-pesq>.
- Zhou Wang, Alan C Bovik, Hamid R Sheikh, and Eero P Simoncelli. Image quality assessment: from error visibility to structural similarity. *IEEE transactions on image processing*, 13(4):600–612, 2004.